JURNAL TEKNIK SIPIL DAN LINGKUNGAN| EISSN:2549-1407
https://jurnal.ipb.ac.id/index.php/jsil

Vol. 09 No. 01 April 2024
DOI: 10.29244/jsil.9.1.51-60

Schiff Base Synthetic Coating from Chitosan Acylation of Green Mussel Shell (*Perna viridis*) as A Corrosion Inhibitor in Reinforcing Steel

Wisely Lukvy, Arief Sabdo Yuwono, Heriansyah Putra*

Department of Civil and Environmental, IPB University, Dramaga, Bogor, 16618 Indonesia
***Correspondence:** heriansyahptr@apps.ipb.ac.id

Abstract: Reinforced concrete is widely used in building construction implementation worldwide. The use of reinforcing steel as a structural material has the potential to experience corrosion. A Schiff base is one of the compounds considered a potential corrosion inhibitor. Green mussel (*Perna viridis*) contains chitosan which can produce chitosan Schiff base. This study aimed to analyze chitosan, Schiff base, optimum inhibitor concentration, and morphological structure. The study consisted of extraction of green clamshell chitosan, acylation transformation stages using Fourier transform infrared (FT-IR), dan UV-Vis Spectrophotometer, corrosion rate measurement using the wight losh method, and morphological structure testing using scanning electromagnetic (SEM). This research resulted in the degree of deacetylation of chitosan from the FT-IR spectra of 53.71%. Chitosan Schiff base from green mussel shells was successfully synthesized as much as 188.41 g. The optimum corrosion rate is found at the inhibitor concentration of 1500 ppm, with the highest efficiency level of 91.84%. The results of SEM testing on treated steel samples yielded fewer corrosion products in the form of uniform corrosion and pitting corrosion than untreated steel samples. This result shows that the chitosan Schiff base inhibitor from the optimum concentration of green mussel shells of 1500 ppm effectively inhibits the corrosion rate.

Keywords: chitosan, corrosion, green mussel shells, reinforcing steel, *Schiff* base

Submitted: 08 Marc 2024
Revised: 02 April 2024
Accepted : 08 April 2024

1. Introduction

Reinforced concrete is widely used in the implementation of construction in Indonesia. Reinforced concrete is chosen because it has a higher structural strength than ordinary concrete. It is due to the reinforcement steel component added to manufacturing reinforced concrete. However, reinforcing steel as a structural material has the potential for corrosion. The negative impact of corrosion on reinforcing steel is the shrinkage of the reinforcing steel area so that the service life of the reinforcing steel is reduced [1-3].

Corrosion prevention has been widely practiced, including by painting metal surfaces using inhibitors [4-6]. Generally, corrosion inhibitors are made from organic compounds that have nitrogen (N), oxygen (O), phosphorus (P), sulfur (S) atoms, and other atoms that have free electron pairs so that they can form complex compounds when applied with metals and amine compounds [7-9]. A Schiff base is one compound that is considered to have potential as a corrosion inhibitor because its use can form electrostatic attraction forces and free electron

bonds. *Schiff* bases from chitosan can be used as inhibitors because they contain the -OH and -NH functional groups. These functional groups contain many unstable free electron pairs and can bind directly to metals [10-12].

Chitosan is a chitin-derived compound found in many shells, one of which is the shell of green mussels (*Perna viridis*) [13-15]. According to WWF Indonesia (2019), the average production of green mussels from 2014 to 2018 was 15345 tons annually, with 70% of that weight being the weight of green mussel shells, which was 10742 tons [16]. One of the areas with abundant green mussel populations is the Cilincing Waters of North Jakarta Bay. The high amount of green mussel production is proportional to the shell waste produced. Generally, green mussel shell waste is only used to make ornaments, cosmetic mixtures, and animal feed [17-18].

The abundance of green mussel shell waste and the potential of green mussel shell chitosan *Schiff* base as a corrosion inhibitor prompted this research topic. Therefore, further research needs to be conducted on the effectiveness of *Schiff* base chitosan in green mussel shells as a corrosion inhibitor on steel reinforcement. This research is expected to increase the effectiveness of steel as a reinforcement material and make maximum use of green mussel shell waste.

2. Materials and Method

2.1. Material

The tools used in the implementation of the research are magnetic stirrer, glass beaker (1000, 250, 100, 50) mL, vacuum, sieve shaker, analytical balance, Fourier Transform Infrared (FT-IR), UV-VIS Spectrophotometer, oven, and SEM (Scanning Electron Microscope). Materials used in the study include green mussel shells, NaOH, *acetic acid, 4-dimethylamino benzaldehyde, ethanol*, HCl, NaCl, *acetone*, quality steel BJTP-280 diameter 10 mm, resin, and anti-corrosion paint.

2.2. Research Procedures

The research data were obtained through four stages, namely the extraction of green mussel shells into chitosan, the acylation transformation of chitosan into chitosan *Schiff* base, testing the corrosion rate using the weight loss method, and testing the morphological structure on the surface of steel samples using SEM (Scanning Electron Microscope).

2.2.1 Extraction of Green Clam Shell Chitosan

The chitosan extraction stages were carried out using Harjanti's method [19]. In the first stage, the green mussel shells were cleaned, pulverized using a blender, then dried for 24 hours in an oven at 100°C. The next deproteination stage was carried out by soaking the green mussel shell powder obtained in 4% NaOH (1: 10 b/v). The demineralization stage begins by putting the residue of the deproteination stage into a 600 mL glass beaker and then adding 1 M HCl (1:15 b/v). The deacetylation stage starts by placing the chitin from the demineralization stage into a 250 mL glass beaker and adding 50% NaOH (1:15 b/v). The chitosan obtained was then oven-dried for 24 hours at 80°C.

2.2.2 Chitosan Acylation Transformation

The acylation transformation of chitosan from green mussel shells into *Schiff* base chitosan was carried out according to the research of Sitanggang *et al*. [20]. The chitosan extracted in the previous stage was weighed as much as 1.2g. The chitosan was then dissolved into 63 mL of 0.15 mol/L *acetic acid* and stirred using magnetic stirring for 3 hours at 25°C. Then, *p-dimethylamino benzaldehyde* of as much as 1.13 g was weighed and dissolved in 10 mL of ethanol. Then, the result *p-dimethylamino benzaldehyde* was added to the result chitosan that had been dissolved in glacial *acetic acid* slowly, stirred with magnetic stir, and refluxed for 24 hours at 60°C. The reaction results were filtered, then rinsed with

distilled water, followed by a rinse with ethanol (p.a). The reaction results were then poured into a Petri dish and dried using an oven for 24 hours at 60°C.

2.2.3 Corrosion Rate Testing using the Weight Loss Method

Measurement of corrosion rate utilizing the weight loss method with ASTM G1-03 [21] and ASTM G31-72 [22] standards. The corrosion rate measurement uses samples with variations in NaCl concentration, inhibitor concentration, and sample immersion time in a test medium that is supplied with air using an aerator for two replicates. After the immersion is complete, the sample is removed and cleaned of rust. Determination of corrosion rate using **Equation (1)**. Determination of inhibitor efficiency on the test samples using **Equation (2)**.

$$\mathrm{Cr} = \frac{3{,}45\times10^{6}\times(\mathrm{W_1}-\mathrm{W_2})}{\mathrm{A}\times\mathrm{T}\times\mathrm{D}} \quad \textbf{(1)}$$

with,

Cr	: Corrosion rate (mpy)	A	: Area of exposure (cm^2)
W_1	: Initial weight (gram)	T	: Exposure time (jam)
W_2	: Final weight (gram)	D	: Density (g/cm^3)

$$EI = \frac{CRo-CR}{CRo}\,x\;100\% \quad \textbf{(2)}$$

with,

EI	: Efficiency (%)
Cro	: Corrosion rate without inhibitor (mpy)
CR	: Corrosion rate with inhibitor (mpy)

2.2.4 Morphological Structure Testing

Morphological structure testing on the steel surface was carried out using Scanning Electron Microscope (SEM) on test samples coated with optimum concentration inhibitor and those not coated with inhibitor, as well as steel samples in the initial condition. The test samples were coated with optimum concentration inhibitor, and the uncoated test samples were immersed in 3% NaCl corrosion media for 48 hours of immersion time according to ASTM G31-72 standard. Morphological structure testing on the steel surface was then carried out using SEM (Scanning Electron Microscope) on steel samples immersed in corrosion media and initial condition steel samples.

3. Results and Discussion

3.1 Pre-Modified Green Shell Chitosan

The FT-IR spectra of pre-modified green mussel shell chitosan are shown in **Figure 1**. The resulting FT-IR spectra of green mussel shell chitosan are compared with the FT-IR spectra of standard chitosan presented in **Figure 2** [23], where in the FT-IR spectra of green mussel shell chitosan, there are hydroxyl and amine absorption bands which are characteristic of chitosan. The absorption band appears at wave number 3348.42 $cm^{-1,}$ which shows the overlap of -OH and N-H group vibrations based on the IR spectra of chitosan in **Figure 1**. Based on the IR spectra of the isolated green mussel shell chitosan, an absorption band also appears at wave number 1591.27 $cm^{-1,}$ which shows the N-H bending vibration of NH2. The -CH_3 bending absorption band at wave number 1377.17 cm^{-1} is still visible but with weaker intensity. This indicates that there has been a deacetylation stage, which causes the loss of some methyl groups, -CH_3. C-N vibrations can be identified at wave number 1321.64 cm^{-1} with less intensity, indicating that there are

still a few C-N groups present. $NHCOCH_3$ group. The C-O bond range was identified at wave numbers 1149.57 cm^{-1} and 1072.42 cm^{-1}. The C-O range can be derived from C-O-C or C-O-H.

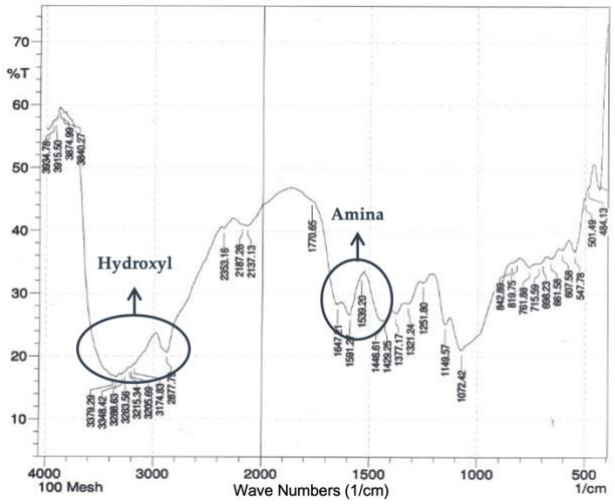

Figure 1. FT-IR Spectra of Pre-Modified Green Shell Chitosan

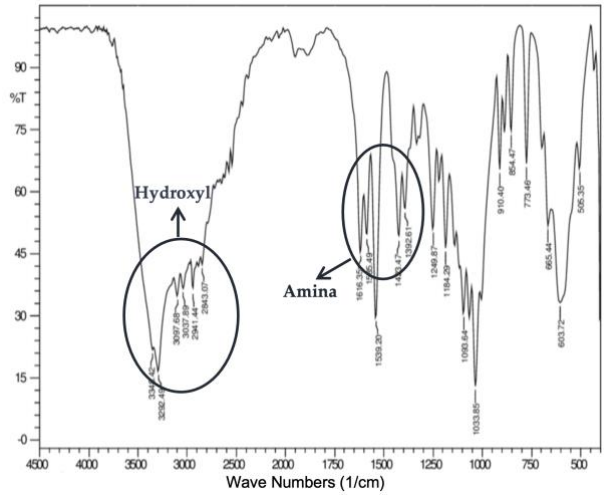

Figure 2. FT-IR Spectra of Standard Chitosan

The degree of deacetylation successfully synthesized from chitosan was 53.71%. The degree of deacetylation obtained is not as high as the chitosan commonly sold in the market (commercial chitosan), but the value of the degree of deacetylation above 50% is optimal enough to be synthesized into *Schiff* base chitosan [24].

3.2 UV-Vis Characterization of Schiff Base Chitosan

The UV-Vis graph of *Schiff* base chitosan, as shown in **Figure 3,** shows the difference in UV absorption of chitosan polymer and *Schiff* base chitosan polymer. *Schiff* base chitosan in solution form shows the peak area (valley) in the 215-325 nm region due to the π bond created. The π bond is an azomethine group (*Schiff* base), C=N [25]. This characteristic region does not exist in ordinary chitosan, which confirms the formation of imine groups in the polymer chain of the modified chitosan as well as in the UV-Vis of chitosan without processing, there is no specific absorption in the 215-325 nm region so that *Schiff* base chitosan can be applied as a corrosion inhibitor. The value of Schiff base chitosan that was successfully synthesized was 188.41 grams.

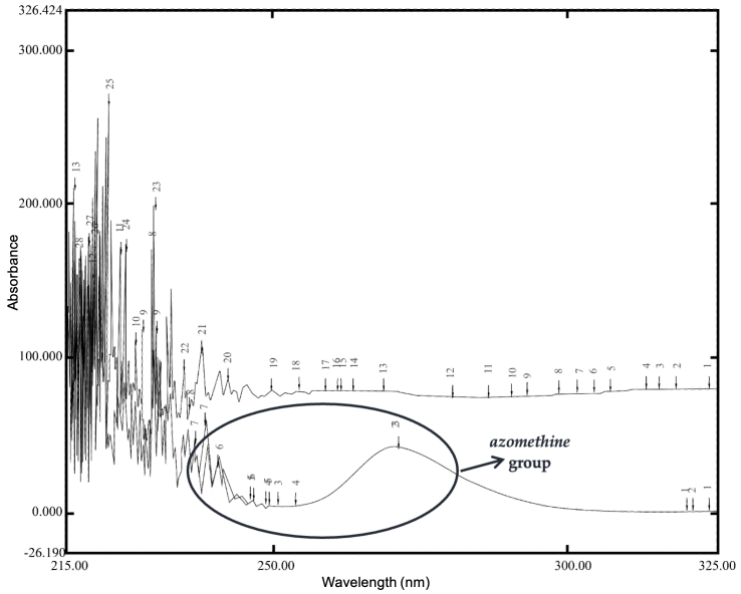

Figure 3. UV-Vis *Schiff* base chitosan

3.3 Corrosion Rate by Weight Loss Method

One way to measure the potential of corrosion inhibitors on reinforcing steel from modified chitosan is by weight loss test. This study used 6 variations of inhibitor concentrations, namely 0 ppm, 500 ppm, 1000 ppm, 1500 ppm, 2000 ppm, 2500 ppm, and anti-corrosion paint as the control variable. The variation of immersion time was carried out for 24 hours, 48 hours, and 72 hours. Variation of corrosion media with 1%, 3%, and 5% concentration NaCl solution. The results of corrosion rate testing using the weight loss method calculated using **Equation (1)** are shown in **Table 1**.

Table 1. Corrosion Rate Test Results

NaCl Concentration (%)	Inhibitor							Soaking time (hour)
	0 ppm	500 ppm	1000 ppm	1500 ppm	2000 ppm	2500 ppm	Anti-corrosion paint	
1	69.19	29.09	17.18	7.91	3.92	2.69	1.05	24
	87.95	63.71	20.91	12.89	5.73	2.87	1.49	48
	97.93	71.89	31.89	16.12	8.71	2.98	1.96	72
3	89.91	33.27	16.09	5.79	3.75	2.77	2.03	24
	106.38	36.98	17.45	8.68	5.57	2.96	2.37	48
	119.93	53.03	33.12	20.73	14.91	7.71	4.13	72
5	119.97	71.17	54.91	31.93	19.76	11.96	7.73	24
	131.71	105.67	89.01	63.87	44.73	24.31	13.92	48
	146.73	111.31	103.74	98.75	79.81	48.31	21.39	72

Description: Unit of corrosion rate in mpy

Based on the results of the corrosion rate test in **Table 1**, the inhibitor efficiency in the test sample was then calculated using **Equation (2)** to obtain the inhibitor efficiency value, as presented in **Table 2**.

Table 2. Inhibitor Efficiency

NaCl Concentration (%)	Inhibitor							Soaking time (hour)
	0 ppm	500 ppm	1000 ppm	1500 ppm	2000 ppm	2500 ppm	Anti corrosion paint	
1	0	57.96	75.17	88.57	94.33	96.11	98.48	24
	0	27.56	76.23	85.34	93.48	96.74	98.31	48
	0	26.59	67.44	83.54	91.11	96.96	98.00	72
3	0	63.00	82.10	93.56	95.83	96.92	97.74	24
	0	65.24	83.60	91.84	94.76	97.22	97.77	48
	0	55.78	72.38	82.71	87.57	93.57	96.56	72
5	0	40.68	54.23	73.39	83.53	90.03	93.56	24
	0	19.77	32.42	51.51	66.04	81.54	89.43	48
	0	24.14	29.30	32.70	45.61	67.08	85.42	72

Description: Units of inhibitor efficiency in %

In the immersion of 1%, 3%, and 5% NaCl corrosion media, it can be seen that the corrosion rate decreases along with the addition of inhibitor concentration, both in the immersion time range of 24 hours, 48 hours, and 72 hours, based on **Table 1**. The decreasing corrosion rate with the addition of inhibitor concentration indicates that the inhibitor adsorbed on the steel surface will cover the active part that should be corroded by the NaCl solution [26]. The decrease in corrosion rate, the increase in efficiency, and the addition of inhibitor concentration indicate that the *Schiff* base inhibitor has potential as a corrosion inhibitor

on reinforcing steel. Furthermore, a graph of the relationship between corrosion rate and inhibitor concentration was made based on variations in NaCl concentration of 1%, 3%, and 5%.

In 1% NaCl immersion, as shown in **Figure 4**, *Schiff* base corrosion inhibitors play an optimal role at concentrations of 1000-2500 ppm in the immersion time range of 24 hours and at inhibitor concentrations of 1500-2500 ppm in the immersion time range of 48 hours and 72 hours. Corrosion inhibitors play an optimal role because the CR (Corrosion Rate) value is less than 20 mpy [27]. Additional tests were also conducted on test samples coated with anticorrosive paint as a control variable. Based on the single factor ANOVA statistical test and the least significant difference statistical test, the corrosion rate with the highest inhibitor concentration, 2500 ppm, is not significantly different from the corrosion rate of anticorrosive paint. The BNT obtained was 5.31 with a standard deviation of 37.57 mpy. The highest efficiency was found in the 72-hour immersion time range, which amounted to 96.96%.

In immersion in 3% NaCl corrosion media, as shown in **Figure 5**, the lowest corrosion rate was obtained in each immersion time range, namely the inhibitor with a concentration of 2500 ppm. The highest efficiency value is found in the 48-hour immersion time range, which is 97.22%. Based on the single factor ANOVA statistical test and the least significant difference statistical test, the corrosion rate with inhibitor concentrations of 1500 ppm, 2000 ppm, and 2500 ppm is not significantly different from the corrosion rate of anti-corrosive paint. The BNT obtained was 6.32 with a standard deviation of 37.55 mpy.

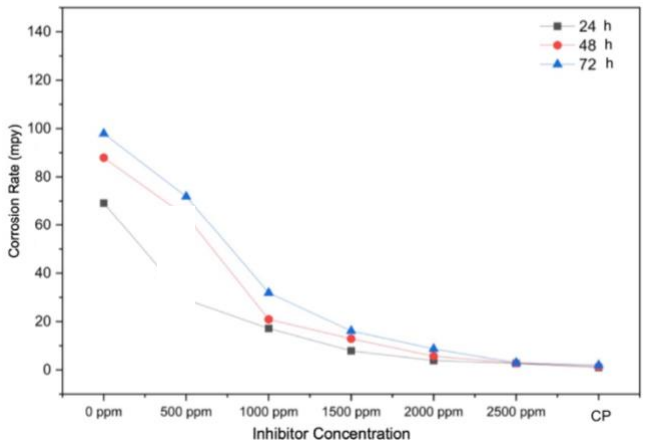

Figure 4. Corrosion Rate of 1% NaCl Immersion

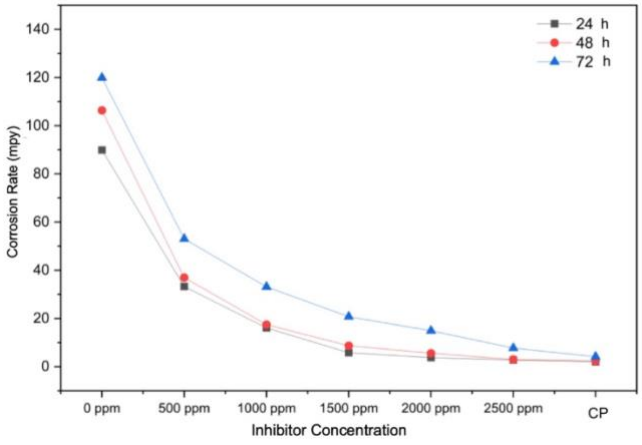

Figure 5. Corrosion Rate of 3% NaCl Immersion

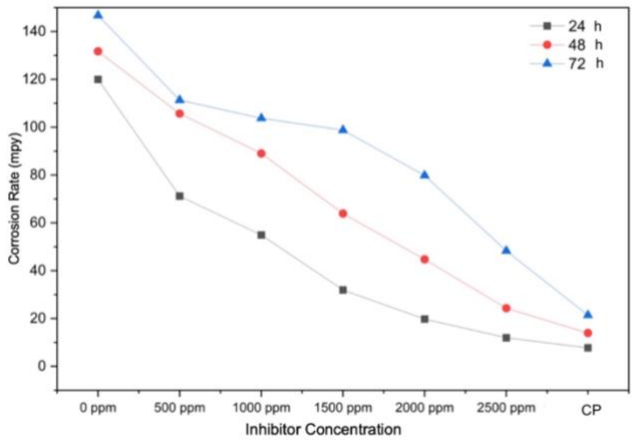

Figure 6. Corrosion Rate of 5% NaCl Immersion

In immersion, in 5% NaCl corrosion media, as shown in **Figure 6**, the corrosion rate tends to be higher than in immersion in 1% and 3% NaCl corrosion media. The resulting efficiency tends to be smaller than

the 1% and 3% NaCl immersion. The resulting efficiency decreases as the immersion period increases [26]. Based on the corrosion rate and efficiency that has been obtained, it is known that the optimum corrosion rate is at an inhibitor concentration of 1500 ppm with an immersion period of 48 hours and 3% NaCl corrosion media following ASTM G31-72 [22].

The optimum corrosion rate is found in inhibitors with a concentration of 1500 ppm because as the inhibitor concentration increases above 1500 ppm, the resulting decrease in corrosion rate is relatively small. This is not directly proportional to the addition of *Schiff* base at inhibitor concentrations of 2000 ppm and 2500 ppm, which reached four times. The optimum inhibitor concentration produced a greater corrosion rate than the corrosion rate of the anticorrosive paint. However, the corrosion rate produced by the optimum inhibitor concentration can work optimally because it has a corrosion rate below 20 mpy [27]. In addition, in terms of price, organic inhibitors in this study have the advantage of utilizing waste, while commercial paints and inorganic inhibitors have relatively high selling prices. The use of organic inhibitors is more environmentally friendly than inorganic inhibitors containing chromate and zinc [28].

3.4 Morphological Structure by SEM (scanning electromagnetic)

Morphological structure testing with scanning electromagnetic (SEM) was conducted on untreated steel samples (without inhibitor) and treated steel samples (optimum inhibitor concentration of 1500 ppm). The steel samples were immersed in 3% NaCl corrosion media for 48 hours based on ASTM G31-72 [22]. SEM results on the surface of steel samples with 1000x magnification are shown in **Figure 7**.

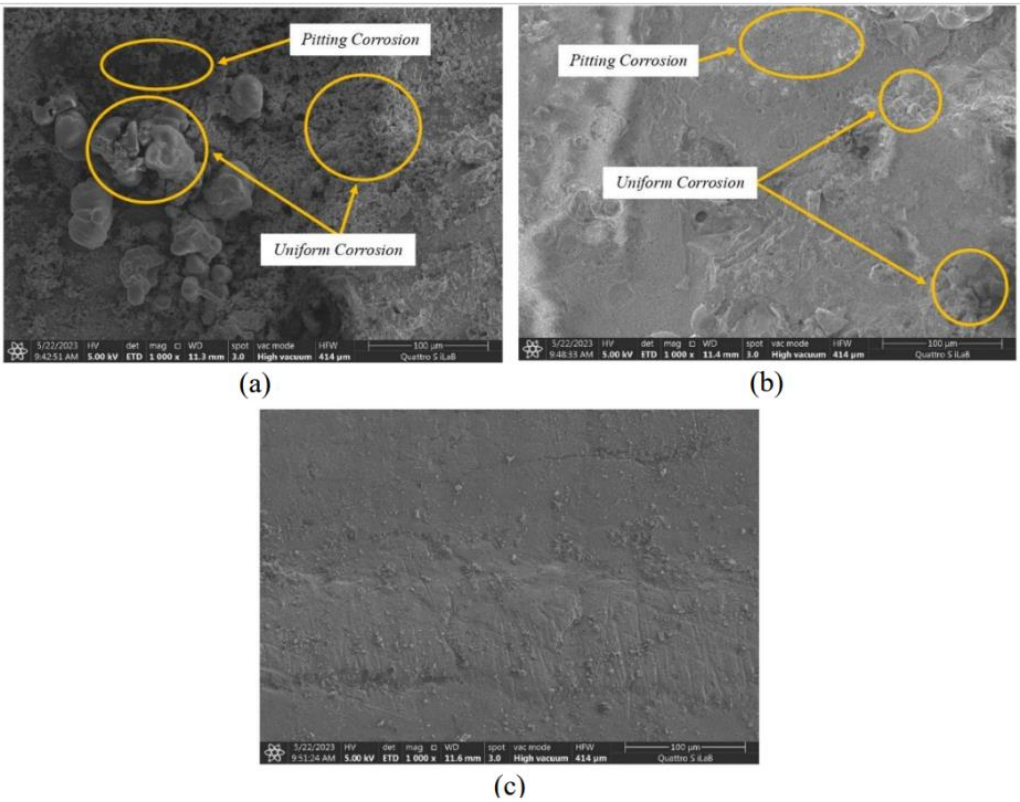

Figure 7. SEM Test Results: (a) Untreated Steel Sample (No Inhibitor), (b) Treatment Steel Sample (Optimum Inhibitor Concentration 1500 ppm), (c) Initial Condition Steel Sample (Initial)

SEM results on untreated steel samples (without inhibitor) in **Figure 7 (a)** show the presence of corrosion products in the form of blobs and holes that cover the entire surface of the steel sample, while on treated steel samples (optimum inhibitor concentration of 1500 ppm) in **Figure 7 (b)** show the presence of corrosion products in the form of blobs and holes with a smaller amount and do not cover the entire surface of the steel sample. Corrosion products on steel samples in the form of blobs are uniform corrosion

products. Uniform corrosion is a corrosion product that occurs on the surface of steel samples due to chemical reactions between steel samples and water and humid environmental air, so the longer the steel sample is thinning [29].

Other corrosion products, namely pits on the surface of the steel sample, are well-corrosion products. Pitting corrosion is a corrosion product that occurs due to the presence of chloride and hydrogen ions from the environment on the surface of steel samples. Oxygen will attach to the surface of the steel sample, thus creating a difference in cell concentration. The part of the steel sample surface in direct contact with oxygen will become a cathode that will bind electrons from the surface that is not in direct contact with oxygen. The part of the surface that is not directly related to oxygen will act as an anode and will lose its electrons. Furthermore, chloride ions and hydrogen ions will be bound to the surface of the steel sample that is not in direct contact with oxygen to stabilize the electrons. The process will produce pits on the surface of the steel sample called pitting corrosion [29-30].

There are pretty clear differences based on the SEM results of the treatment steel samples (optimum inhibitor concentration of 1500 ppm) and untreated steel samples (without inhibitor). In the treatment steel sample (optimum inhibitor concentration of 1500 ppm), it can be seen that the corrosion products formed are less than the corrosion products produced in the untreated steel sample (without inhibitor). Morphological structure testing with SEM (Scanning Electron Microscope) was also performed on the initial steel samples without soaking them and without coating them with an inhibitor for comparison. The surface of the initial steel sample in **Figure 7 (c)** does not show any corrosion products in the form of lumps and pits, indicating that corrosion has not occurred on the steel sample.

Based on the results obtained from SEM testing, it is known that the morphological structure of the treated steel sample (optimum inhibitor concentration of 1500 ppm) is close to the morphological structure of the initial steel sample that has not yet encountered corrosion. This shows that the chitosan *Schiff* base inhibitor from green mussel shells at the optimum concentration (1500 ppm) works well in inhibiting the corrosion rate of steel samples. This result indicated that the optimum concentration of *Schiff* base inhibitor (1500 ppm) adsorbed on the steel surface covers the active part of the surface that should be corroded by NaCl solution [26].

4. Conclusion

Green mussel shell waste can be utilized to serve as an alternative corrosion inhibitor coating on reinforcing steel. Green mussel shell chitosan was successfully obtained from the extraction process with a deacetylation degree of 53.71%. *Schiff* base chitosan was successfully obtained from the acylation transformation characterized by the formation of azomethin groups. The optimum chitosan *Schiff* base inhibitor is found at a concentration of 1500 ppm with a resulting corrosion rate of 8.68 mpy and an efficiency of 91.84%. The treatment steel sample shows corrosion products in the form of uniform corrosion, and pitting corrosion is formed less than in the untreated steel sample. In addition, the morphological structure of the treatment steel sample is close to the morphological structure of the initial steel sample that has not yet encountered corrosion. This shows that the chitosan *Schiff* base inhibitor from green mussel shells at the optimum concentration (1500 ppm) works well in inhibiting the corrosion rate of steel samples.

References

[1] Amalia Z, Saidi T, Aulia TB, Mahlil. Effect of current density on the cracking behavior of reinforced concrete subjected to reinforcement corrosion. *Journal of Teras.* 2021; 11(2): 351−362.

[2] Quraishi MA, Nayak DK, Kumar R, Kumar V. Corrosion of reinforced steel in concrete and its control: an overview. *Journal of Steel Structures & Construction*. 2017; 3(1): 1−6.

[3] Yu B, Liu J, Chen Z. Probabilistic evaluation method for corrosion risk of steel reinforcement based on concrete resistivity. *Journal of Construction and Building Materials*. 2017; 138(1): 101−113.

[4] Saugi W. Effect of physical, chemical, and biological factors of the medium on the corrosion rate of iron. *Borneo Journal of Science and Mathematic Education*. 2021; 1(1): 33−60.
[5] Verma C, Ebenso EE, Bahadur I, Quraishi MA. An overview on plant extracts as environmental sustainable and green corrosion inhibitors for metals and alloys in aggressive corrosive media. *Journal of Molecular Liquids*. 2018; 266(1): 577−590.
[6] Verma C, Ebenso EE, Quraishi MA. Ionic liquids as green and sustainable corrosion inhibitors for metals and alloys: an overview. *Journal of Molecular Liquids*. 2017; 233(1): 403−414.
[7] Aditama RY, Ginting E, Syafriadi. Effectiveness of papaya leaf extract (*Carica papaya l*) as an inhibitor on AISI 1020 carbon steel in 3% NaCl corrosive medium. *JTAF.* 2019; 7(1): 69−76.
[8] Sedik A, Lerari D, Salci A, Athmani S, Bachari K, Gecibesler IH, Solmaz R. Dardagan fruit extract as eco-friendly corrosion inhibitor for mild steel in 1 M HCL: electrochemical and surface morphological studies. *Journal of the Taiwan Institute of Chemical Engineers*. 2020; 107(1): 189−200.
[9] Tan B, He J, Zhang S, Xu C, Chen S, Liu H, Li W. Insight into anti-corrosion nature of betel leaves water extracts as the novel and eco-friendly inhibitors. *Journal of Colloid and Interface Science*. 2021; 585(1): 287−301.
[10] Stiadi Y, Arief S, Aziz H, Efsi, Mai, Emriadi. Corrosion inhibition of mild steel using natural materials in hydrochloric acid medium. *JKR.* 2019; 10(1): 51−65.
[11] Ansari KR, Chauhan DS, Quraishi MA, Mazumder MAJ, Singh A. Chitosan Schiff base: an environmentally benign biological macromolecule as a new corrosion inhibitor for oil & gas industries. *International Journal of Biological Macromolecules*. 2020; 144(1): 305−315.
[12] Messali M, Larouj M, Lgaz H, Rezki N, Al-Blewi FF, Aouad MR, Chaouiki A, Salghi R, Chung IM. A new schiff base derivative as an effective corrosion inhibitor for mild steel in acidic media: experimental and computer simulations studies. *Journal of Molecular Structure*. 2018; 1168(1): 39−48.
[13] Arsyi NZ, Nurjannah E, Nurahlina D, Budiyanti E. Characterization of nano chitosan from green mussel shells by ionic gelation method. *JTBA.* 2018; 2(2): 106−111.
[14] Harmami H, Ulfin I, Sakinah AH, Ni'mah YL. Water-soluble chitosan from shrimp and mussel shells as corrosion inhibitor on tinplate in 2% NaCl. *Malaysian Journal of Fundamental and Applied Sciences*. 2019; 15(2): 212−217.
[15] Thilagar G, Sasikumar T, Arumugam R, Samuthirapandian R. Preparation and characterization of chitosan from *Perna viridis* (Linnaeus, 1758) shell waste as raw material. *Research Journal of Pharmacy and Technology*. 2021; 14(5): 2757−2762.
[16] [WWF] World Wide Fund for Nature Indonesia. 2019. *Indonesian Fisheries and Marine Products Production Catalog 2014-2018*. Jakarta: WWF Indonesia Fisheries Team.
[17] A'yuni Q, Widianti A, Ulfindrayani IF, Prayogi YR, Arif S, Ningsih AFL. Utilization of clam shell waste as quality animal feed in Tambak Cemandi Village, Sidoarjo. *JSSD*. 2019; 2(2): 61−69.
[18] Ismail R, Fitriyana DF, Santosa YI, Nugroho S, Hakim AJ, Mulqi MSA, Jamari J, Bayuseno AP. The potential use of green mussel (*Perna Viridis*) shells for synthetic calcium carbonate polymorphs in biomaterials. *Journal of Crystal Growth*. 2021; 572(1): 126−133.
[19] Harjanti RS. Chitosan from shrimp waste as a preservative for fried chicken. *J. Rek. Pros*. 2018; 8(1): 12−19.
[20] Sitanggang BC, Wirjosentono B, Ginting M. Preparationof fe-chitosan *schiff* base complex. *Journal of Chemical Education*. 2018; 8(3): 203−206.
[21] [ASTM] American Society for Testing and Materials. ASTM G1-03:2017 *Standard Practice for Preparing, Cleaning, and Evaluating Corrosion Test Specimens*. 2017.
[22] [ASTM] American Society for Testing and Materials. ASTM G31-72:2013 *Standard Practice for Laboratory Immersion Corrosion Testing of Metals*. 2013.

[23] Zaeni A, Safitri E, Fuadah B, Sudiana IN. Microwave-assisted hydrolysis of chitosan from shrimp shell waste for glucosammine hydrochlorid production. *Journal of Physics: Conference Series*. 2017; 846(1): 1−8.

[24] Komi DEA, Hamblin M. Chitin and chitosan: production and application of versatile biomedical nanomaterials. *International Journal of Advanced Research*. 2016; 4(3): 411−427.

[25] Sirumapea L, Asmiyanti, Khoirunisa A. Synthesis and characterization of antibacterial compounds Fe(III) complexes with schiff base derivatives. *IJPST*. 2015; 2(2): 49−54.

[26] Priyotomo G, Sitepu HS, Dwiyanti Y. Effect of adding taro leaf extract inhibitor concentration on the corrosion rate of 5L X-52 fire steel in 0.5 M H_2SO_4 solution. *Widyariset*. 2019; 5(1): 30−36.

[27] Arif MN, Sinardi, Soewondo P. Comparative study of green mussel shell and crab shell chitosan by chemical preparation as natural coagulant. *JTLITB*. 2013; 19(1): 64−74.

[28] Bahlakeh G, Ramezanzadeh B, Ramezanzadeh M. The role of chrome and zinc free-based neodymium oxide nanofilm on adhesion and corrosion protection properties of polyester/melamine coating on mild steel: experimental and molecular dynamics simulation study. J*ournal of Cleaner Production*. 2019; 210(3): 872−886.

[29] Pessu F, Hua Y, Barker R, Neville A. A study of the pitting and uniform corrosion characteristics of X65 carbon steel in different H2S-CO2-containing environments. *The Journal of Science and Engineering*. 2018; 74(8): 886−902.

[30] Grachev V, Rozen AA, Vasilievich G. Mechanism of pitting corrosion protection of metals and alloys. *Oriental Journal of Chemistry*. 2016; 32(2): 845−850.